Technical Report ARAED-TR-90038

FRACTURE OF COMPOSITION B AND TNT

D. A. Wiegand
J. Pinto

April 1991

U.S. ARMY ARMAMENT RESEARCH, DEVELOPMENT AND ENGINEERING CENTER

Armament Engineering Directorate

Picatinny Arsenal, New Jersey

REPORT DOCUMENTATION PAGE

Form Approved
OMB NO. 0704-0188

1. AGENCY USE ONLY *(Leave blank)*	2. REPORT DATE	3. REPORT TYPE AND DATES COVERED
	April 1991	

4. TITLE AND SUBTITLE

FRACTURE OF COMPOSITION B AND TNT

5. FUNDING NUMBERS

6. AUTHOR(S)

D. A. Wiegand and J. Pinto

7. PERFORMING ORGANIZATION NAME(S) AND ADDRESS(ES)

ARDEC, AED
Energetics and Warheads Division (SMCAR-AEE)
Picatinny Arsenal, NJ 07806-5000

8. PERFORMING ORGANIZATION REPORT NUMBER

Technical Report ARAED-TR-90038

9. SPONSORING/MONITORING AGENCY NAME(S) AND ADDRESS(ES)

ARDEC, IMD
STINFO Br
ATTN: SMCAR-IMI-I
Picatinny Arsenal, NJ 07806-5000

10. SPONSORING/MONITORING AGENCY REPORT NUMBER

11. SUPPLEMENTARY NOTES

12a. DISTRIBUTION/AVAILABILITY STATEMENT

Approved for public release; distribution is unlimited.

12b. DISTRIBUTION CODE

13. ABSTRACT ***(Maximum 200 words)***

The compressive fracture strength of Composition B and TNT has been investigated in uniaxial compression as a function of temperature and strain rate. Young's modulus and other aspects of stress strain behavior were also studied. The compressive fracture strengths and the moduli decrease with increasing temperature and decreasing strain rate. Limited tensile measurements were also made. Failure is by brittle fracture for all conditions investigated and can be explained in terms of the Griffith criteria for fracture. The temperature and strain rate dependence of the compressive strength can be attributed to the dependence of the modulus on these parameters and thermally activated slow subcritical crack growth before fracture.

14. SUBJECT TERMS

Composition B, TNT, Fracture, Uniaxial stress, Compressive strength, Cracking, Tensile strength, Crack propagation, Slow crack growth, Sub-critical crack growth, Grain boundary sliding, Bond breaking, Activation energy, Apparent modulus

15. NUMBER OF PAGES

40

16. PRICE CODE

17. SECURITY CLASSIFICATION OF REPORT	18. SECURITY CLASSIFICATION OF THIS PAGE	19. SECURITY CLASSIFICATION OF ABSTRACT	20. LIMITATION OF ABSTRACT
UNCLASSIFIED	UNCLASSIFIED	UNCLASSIFIED	SAR

ACKNOWLEDGMENTS

The authors are indebted to D. Georgevich and M. Mezger for assistance with data taking and to M. Mezger and Y. Lanzerotti for helpful discussions. The authors also wish to thank C. Ribaudo for material characterization, G. Ziegler for casting TNT and Comp B, J. Jenkins for the machining of samples and F. Glanzel for radiographic work.

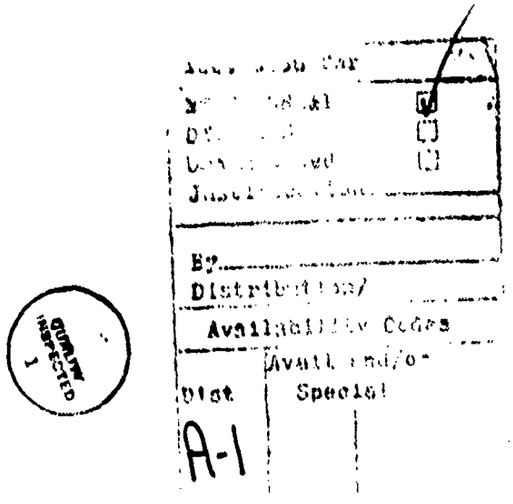

CONTENTS

FIGURES

INTRODUCTION

Little attention has been given to determining and understanding the mechanical properties of composite explosives. In an effort to understand these types of materials and, in particular, to determine and understand failure conditions, the mechanical properties of trinitrotoluene (TNT) and Composition B (Comp B), a composite of TNT and cyclotrimethylene trinitramine (RDX) have been investigated. Measurements have been made as a function of temperature and strain rate. Both TNT and Comp B are very important military explosives. Knowledge of the mechanical properties and, in particular, the conditions for failure are very important relative to the safe use of these materials. The conditions of stress, strain rate, and temperature experienced during cast cooling, handling, and in weapons use such as artillery launch, are of special importance. Thus, studies were made for two strain rates, a quasi-static rate which is appropriate for cast cooling and some handling conditions, and a higher strain rate which is applicable to other conditions of handling and weapons use. Temperatures between 0° and 60°C were used in the studies reported in this paper. The majority of measurements were made in compression and the results for uniaxial compression are reported here. Very limited measurements were also made in uniaxial tension. Studies have also been made for triaxial confined compression and the results of these studies will be given in a companion report (ref 1). The triaxial confined conditions simulate the conditions which the explosives experience during artillery launch.

TNT and Comp B were prepared by casting from the melt. Comp B can be prepared by adding particulate RDX and wax to molten TNT. Comp B contains 39.4% TNT, 59.6% RDX, and 1% wax. TNT and Comp B fail by brittle fracture under uniaxial loading and these materials are much weaker in tension than in compression. During the casting and cooling process defects such as cracks, porosity, and larger voids or cavities are often introduced. These defects are very important because they are thought to play a critical role in, for example, premature ignition during artillery launch. Some of these defects are caused by stresses during cast cooling, e.g., thermal stresses, and mechanical properties for these conditions are needed for computer modeling so as to be able to predict conditions which will not result in defect generation. There are free surfaces because of these defects and so measurements were made for the simplest conditions of free surfaces, i.e., uniaxial stress and at a low quasi-static rate. Measurements were also made at a higher strain rate to provide the information and understanding necessary for computer modeling in order to predict failure conditions with defects during use, e.g., during artillery launch.

Complete stress versus strain curves were recorded as a function of the various parameters mentioned above and particular attention has been given to the compressive strength, Young's modulus, and also the strain at the compressive strength. The goal is to develop a basic understanding of these materials which will enable predictions

of failure conditions and provide guidance for avoiding failure. Limited numbers of measurements were made for each condition of temperature and strain rate. The intent was to survey the mechanical properties as a function of these conditions to provide the bases for an understanding. Additional work with larger numbers of samples is desirable to place the results and understanding presented here on a firmer base.

Finally, it is important to note that at no time during the course of these experimental studies was any evidence of fast explosive reaction observed.

EXPERIMENTAL

Some preparation and the loading apparatus are described in detail elsewhere and only a few comments are given here (ref 2). These are concerned with the calibrations of the loading apparatus sensors and the strain rate as a function of time.

A linear variable differential transformer (LVDT) was used to measure the displacement of the actuator rod and thus the change in length of the sample. A load cell was used to measure the applied force. The LVDT and the load cell were calibrated annually by the manufacturer. Additional static calibrations of the LVDT were made with a machinist type dial indicator gage using increments of 0.001 inch. The LVDT was also calibrated dynamically at several strain rates against strain gages using a lucite sample (ref 3). This calibration is of some importance because some of the results presented here are not in agreement with the results of others.

The experiments described here were performed using a medium rate, high load, servo-hydraulic system. At low rates this system is capable of applying constant load (stress) or displacement (strain) rates to the sample and at such rates the acceleration and deceleration of the cross head are not significant. However, when the apparatus is driven to its maximum rate as it was in the work reported here for the high strain rate, the acceleration and deceleration can be significant. In order to avoid deceleration problems, the apparatus was overdriven, i.e., the maximum load or displacement programmed into the computer was greater than that necessary to complete the desired effect, e.g., compressive failure in the uniaxial case. The stress and strain rates were not constant for the high strain rate work since the hydraulics had to be overdriven to obtain the desired strain rate and typical curves of strain rate and stress versus time as given in figure 1. The strain rate data has been smoothed by averaging every nine points of the original strain rate versus time curve. The noise in the strain rate curve originates in the LVDT as well as contributions from analogue to digital and digital to analogue conversions required in the high rate data handling processes. After the initial acceleration the strain rate has the average value of 1.4 s^{-1}. For all data given in this paper, high strain rate refers to the strain rate versus time data of figure 1. The low strain rate was constant at 6.7×10^{-4} s^{-1} to within approximately 1%.

RESULTS

Most of the results presented here were presented previously in slightly modified form. They are presented here for completeness. The objective of this report is to provide a detailed interpretation of the results.

Composition B

Comp B samples, some of which were cast in a split mold and others which were cast in smaller cardboard tubes, were measured in uniaxial compression. The specimens from the smaller cardboard tubes were measured at the low and high strain rates and at 0°, 23°, 40°, and 60°. Measurements were also made at -20° and -40°C but the results were very erratic and nonreproducible, and are not presented. In all of these experiments axial stress and strain were measured and a modulus was calculated from the slope of the stress versus strain curve. Stress versus strain curves for Comp B are given in figures 2 and 3 and photographs of typical sample fragments after failure are given in figure 4. The compressive strength, σ_m, is taken at the maximum of the stress versus strain curve. ε_m is the strain at σ_m, and Young's modulus is taken as the slope of the straight line region as shown. The terms Young's modulus or simply modulus and denoted by E are used throughout when referring to this slope. It is desirable to distinguish between this slope and a true elastic modulus (constant). The sample fragments indicate a brittle type of failure. There is some crumbling and powdering as a result of uniaxial compressive failure (not shown in figure 4). Very extensive powdering has also been found as a result of mechanical failure of a simulated void due to an applied compressive stress (ref 4). In addition, extensive powdering occurred in specimens as a result of impact (ref 5).

The average compressive strength at 23°C and at the high strain rate is 3260 ± 150 psi, the average strain, ε_m, is 0.65 ± 0.10%, and the average Young's modulus is (0.60 ± 0.02) x 10^6 psi. The results at 23°C are summarized in table 1. In general the strains, ε_m, were found to vary more from sample to sample than the moduli or the compressive strengths (ref 2). This variation in the strains at failure is undoubtedly due, as least in part, to uncertainties inherent in the method by which they were determined. Because of the rounding of the stress versus strain curves in the vicinity of σ_m and because of noise in the data there is more uncertainty in the determination of ε_m than in the determination of σ_m from the curves (figs. 2, 3, and 7). Although samples were machined into cylinders with axes parallel and perpendicular to the cast axis, insufficient data were obtained to determine if there was a dependence of these mechanical properties on the orientation of the axis (ref 2). Orientation dependence has been found for low rate measurements (ref 6).

The results of uniaxial measurements of Comp B cast in the small cardboard tubes are given in figure 5 for two strain rates and four temperatures. The low rate compressive strength data agree well with the data of Costain and Motto (ref 8) as a function of temperature and the high rate compressive strength at room temperature is in agreement with the value given by Clark and Schmitt (ref 9). These investigators made measurements on Comp B under similar loading conditions on specimens of comparable size to those used in this study. The results of figure 6 indicate that the uniaxial compressive strength decreases with increasing temperature and decreasing strain rate (figs. 2 and 3). Clark and Schmitt (ref 9) also report a decreasing compressive strength with decreasing rate but they report a considerably greater decrease for a somewhat smaller decrease in rate.

The results presented in figures 2 and 3 indicate that the modulus also decreases with decreasing strain rate. In figure 6 the modulus, E, is given as a function of temperature at the low and high strain rates as determined from the uniaxial measurements. The results indicate that E decreased with increasing temperature and decreasing strain rate. More extensive data obtained by triaxial compression measurements indicate the same dependence on temperature and strain rate (refs 1 and 2). In contrast Clark and Schmitt (ref 9) found no dependence of the modulus on rate. However, in later work of these investigators with more limited data as a function of rate, the modulus at four temperatures was found to be higher at the higher rate (ref 10). There also is some indication that the strains at failure are lower at the low strain rate (ref 2). However, as noted above, there is considerable scatter in the strains, ε_m. Thus, this trend as a function of strain rate cannot be taken as too significant.

Both Clark and Schmitt (refs 9 and 10) and Costain and Motto (ref 8) report moduli which are significantly larger (a factor of two or more) than values reported here. (Larger moduli obtained by other techniques have also been reported elsewhere (ref 11).) While Clark and Schmitt (ref 10) report moduli which decrease with increasing temperature, the more limited data of Costain and Motto (ref 8) indicate an increase in modulus with increasing temperature. Smaller strains at failure are also reported by these investigators. The methods of sample preparation and the quality of the samples used by these investigators are unknown, although Clark and Schmitt do give sample densities and indicate that some samples were vacuum cast (refs 9 and 10). Costain and Motto give only average densities. In addition, the stress versus strain curves given by Clark and Schmitt show considerable curvature and Costain and Motto do not give stress versus strain curves. In the work reported here the stress versus strain curves are linear almost to failure (figs. 2 and 3) and the moduli are determined by the slopes of the linear regions. The load cell and LVDT used in this work were calibrated annually by the manufacturer as noted above and have shown no significant changes over several years.

A few samples of Comp B were strain gaged and measurements made with the same apparatus to determine the modulus, E, and Poisson's ratio, ν (ref 3). In all cases the axial strains as determined by the strain gages are smaller by a factor of two or less than the strains as determined by the LVDT, and thus the E values obtained using the strain gage strains are larger than the E values obtained using the LVDT strains by the same factor. In contrast, the average value of ν obtained from the strain gages for the low strain rate is 0.34 which is approximately in agreement with the value obtained from the triaxial measurements at 23°C (refs 1 and 2). Because of the calibration of the LVDT, the conclusion has been made that the results for the strain gages are in error, most probably because the glue (Eastman 910) did not establish the correct flexible contact between the Comp B and the strain gages. The same fractional error is to be expected for the radial and axial parts of the strain gage. Thus, the value of ν as obtained as a ratio of these strains is found to agree with the value as determined in the triaxial measurements. Clark and Schmitt (refs 9 and 10) used strain gages and report E values which are considerably larger than the values reported in this paper and obtained using the LVDT to measure strain. However, Clark and Schmitt also obtained larger values of E from triaxial data using an LVDT to determine the strains (ref 10).

A very limited number of measurements of Comp B in uniaxial tension were also made. These measurements were made using cylindrical samples of the same type used for the compression studies. The flat ends of the samples were attached to metal cylinders using Eastman 910 adhesive and the metal cylinders were in turn attached to the fixed and movable crossheads using a threaded arrangement. Preliminary measurements were made at the low and high strain rates at 23°C.

The results indicate that Comp B is very weak in tension. Failure in all cases was by brittle fracture and the fracture surfaces were approximately perpendicular to the direction of the applied tensile stress. The tensile strength, σ_t, was found to be 164 ± 21 psi at the low strain rate at 23°C for eight samples. A few other samples gave extremely low values of σ_t and are not included in the above average. This value of σ_t is lower than but close to the value reported by Costain and Motto, i.e., 208 psi at 23°C (ref 8). Only two measurements were made at the high strain rate, and the tensile strengths of these two samples were 470 and 480 psi, respectively. These results indicate a significant increase in tensile strength with increasing strain rate. An increase in tensile strength with increasing strain rate has been report for PETN (ref 12). Although failure was in the explosive (Comp B) and not in the adhesive, many of the samples loaded at both high and low rate failed close to the Comp B-adhesive interface. While no evidence for chemical reaction between Comp B and the adhesive could be detected, it is felt that these tensile measurements should be repeated using the standard dogbone type of samples.

TNT

Experiments similar to those performed on Comp B were performed on TNT. These experiments were carried out to determine the effects of adding RDX and wax to TNT to make Comp B. In addition, TNT is an important material by itself. Military grade TNT was cast in the split mold and in cardboard tubes. Measurements were made as a function of temperature and strain rate as for Comp B, and a typical stress versus strain curve at 23°C. The high strain rate is given in figure 7. At 23°C and the high strain rate the average value of the compressive strength, σ_m, is 1850 ± 180 psi, the average value of the modulus, E, is (0.45 ± 0.07) x 10^6 psi and the average value of ε_m is 0.58 ± 0.07%. Thus, at 23°C and the high strain rate, the average compressive strength and modulus for TNT are smaller than the values for Comp B, but the average strains, ε_m, are not significantly different for the two materials (table 1). In fact, at each temperature and at each strain rate for which measurements were made the compressive strength and the modulus for Comp B are greater than the values for TNT and the strains, ε_m, are approximately the same (ref 2).

The compressive strengths as a function of temperature and rate are summarized in figure 8. σ_m decreases as temperature is increased at both rates. There is also an increase of σ_m for all four temperatures as the rate is increased so that both the temperature and rate dependencies are the same as for Comp B. The low-rate σ_m data are in agreement with the results of Costain and Motto (ref 8). While there is considerable scatter in the modulus values, E does tend to decrease as temperature is increased and does increase as rate is increased (ref 2). Although the E values are smaller than the values reported by Clark and Schmitt (ref 10) the temperature dependence is similar. The E value at 23°C and the low strain rate is also somewhat smaller than the value given by Costain and Motto and the temperature dependence appears to be opposite (ref 8). (The modulus as obtained by other techniques has also been found to be greater than the values reported in this work (ref 13).)

Summary of Experimental Results

The compressive strength and Young's modulus are dependent on temperature and strain rate and a summary of the results at 23°C is given in table 1. The compressive strength and Young's modulus at each temperature and at each strain rate are smaller for TNT than for Comp B while the strains at failure are approximately the same for both materials at each temperature and at each strain rate (ref 2). The compressive strengths and the moduli of TNT and Comp B decrease with increasing temperature and decreasing strain rate. It should be noted, however, that the strain rate sensitivity is

very small, e.g., an increase in the strain rate by a factor of approximately 2.0 x 10^3 results in an increase in the compressive strength by only approximately a factor of two. The increase in the moduli for this change in strain rate is even smaller. The value of the moduli for TNT and Comp B found in this work are smaller than the values reported by other investigators.

DISCUSSION

In the following, a discussion of brittle fracture for both tensile and compressive loading is given and the temperature and strain rate dependencies of the compressive strength are considered. Much more complete data for the Young's modulus will be given in a later report (ref 14). Hence, the discussion of the dependence of the modulus on the above parameters will be given in that report.

Brittle Fracture

Griffith (refs 15 and 16) was the first to suggest that brittle materials contain randomly orientated cracks and that under tensile or compressive loading stress concentrations develop at the crack tips which cause them to propagate and lead to failure by brittle fracture. By applying energetic considerations he obtained an expression for brittle tensile fracture as

$$\sigma_t\sqrt{c} = \left[\frac{2E\gamma}{\pi}\right]^{\frac{1}{2}} \tag{1}$$

where σ_T is the tensile strength, E is Young's modulus (a ture elastic modulus), and γ is surface energy per unit area. Griffith verified this relationship experimentally by studies on glass (ref 15). In addition Griffith showed that tensile stress concentrations occur for applied compressive stresses (ref 16). The relationship between the uniaxial tensile strength, σ_T, and the uniaxial compressive strength, σ_m is given by Griffith as

$$\frac{\sigma_m}{\sigma_T} = 8 \tag{2}$$

While many of the assumptions made by Griffith in obtaining equation 1 are not valid for the experimental conditions used in this work, the ratio given by equation 2 is expected to be of more general validity. In fact, agreement with equation 1 has been found for many materials (ref 17). For Comp B, using the limited tensile strength data presented we have at 23°C for the low strain rate σ_m/σ_T = 9.8 and for the high strain rate σ_m/σ_T = 6.9 in approximate agreement with the Griffith prediction of equation 2. From the data

of Costain and Motto (ref 8) at a low strain rate the ratio σ_m/σ_T is 8.4 for Comp B and 8.0 for TNT at 23°C. For 10 composite explosive formulations with cast TNT as the base (including TNT and Comp B) treated by Costain and Motto this ratio is in the vicinity of 8.0 for most at 23°C, 52°C, and 71°C. At -40°C and -62°C this ratio is higher apparently because of a decrease of the tensile strength with decreasing temperature in this low temperature range. Some difficulty was encountered in making the tensile measurements reported by Costain and Motto at low temperatures because of sample breakage during handling, etc., apparently due to extreme brittleness (ref 18). It is thus possible that the tensile strengths reported by these investigators at the lower temperatures are low because of undetected flaws introduced during handling.

For uniaxial compressive loading the maximum tensile stress will develop at elliptical cracks whose major axis makes an angle of 30 degrees with the direction of the applied stress and for zero thickness cracks the angle between the crack and the applied stresses is 45 degrees (ref 19). These tensile stresses are in such directions that new cracks will initiate and extend toward the direction of the applied compressive stress (ref 19). As the new crack extends it may turn in toward the direction of the applied stress (ref 19). These tensile stresses are in such directions that new cracks will initiate and extend toward the direction of the applied compressive stress (ref 19). As the new crack extends it may turn in toward the direction of the applied stress (ref 19). In this case the stress concentration at the tip will decrease and the crack will stop growing. Alternately, the new crack, which has its own stress concentration, may branch, i.e., initiate another new crack which will also extend in the direction of the applied stress. By continued branching, a network of cracks will develop which will eventually be connected and result in fracture of the specimen into columns aligned in the direction of the applied stress. An inspection of figure 4 will reveal that this type of fracture behavior is observed for Comp B in uniaxial compression. The rounding of the stress versus strain curves just before the rapid decrease of stress which indicates fracture may be due to this initiation, growth and arrest of cracks (figs. 2, 3, and 7). In some other cases the fracture surfaces for Comp B have been diagonal but the frequency of these occurrences have not been studied. This behavior may be due to the effect of frictional forces between the ends of the sample and the crosshead surfaces.

The Griffith theory is based on a two-dimensional model, i.e., a crack in a thin plate. However, the problem has been considered in three dimensions for a penny shaped crack (ref 20). The results indicate that the boundary stresses at the crack and the surface energy differ from those of the two-dimensional case by only a few percent.

In summary, the Griffith theory of crack growth leading to fracture adequately explains the observed ratios of compressive to tensile strengths for Comp B and TNT. In addition, this approach predicts the observed orientation of the fracture surfaces.

The cracks may be in the material before loading and could be caused, for example, by thermal stresses during cooling from the melt, or they may be generated during plastic deformation by slip processes and interactions of dislocations (ref 21).

Role of the Temperature and Strain Rate Dependencies of the Modulus and Surface Energy

An inspection of figures 5 and 8 reveals that the compressive strengths of Comp B and TNT are functions of both temperature and strain rate. While the number of samples measured is small, it is believed that the results of figures 5 and 8 give a true picture of the trend of the compressive strengths with temperature and strain rate. The results at the low strain rate are in good agreement with the results of Costain and Motto (ref 8). Based on the Griffith theory of fracture (eq 1) the temperature and strain rate dependencies of the fracture strength must be due to the temperature and strain rate dependencies of either or both, γ, the surface energy per unit area, and E, Young's modulus, since the crack length, 2c, is assumed to be independent of temperature. From figure 8, we note the E as determined by the slope of the stress versus strain curve is a function of temperature and strain rate for Comp B and more limited data shows that E for TNT (ref 2) also is a function of temperature and strain rate. Assuming for the moment that γ is independent of temperature, and further that E as determined from the slope is a true elastic modulus, we find from equations 1 and 2 that

$$\frac{\Delta\sigma_m}{\sigma_{m_1}} = \left[1 - \left(1 - \frac{\Delta E}{E_1}\right)^{\frac{1}{2}}\right] \tag{3}$$

where $\Delta\sigma_m = \sigma_{m_1} - \sigma_{m_2}$ is the difference in σ_m for two temperatures at constant strain rate or the difference in σ_m for two strain rates at constant temperature. $\Delta E = E_1 - E_2$ is the difference in E for two temperatures at constant strain rate or the difference in E for two strain rates at constant temperature. By using data from figures 5, 6, and 8 and reference 2 we find for both Comp B and TNT that $\Delta\sigma_m/\sigma_m$ as measured is significantly greater than $\Delta\sigma_m/\sigma_{m_1}$ as calculated from equation 3 for changes of either temperature or strain rate. It thus seems necessary at this point to conclude that the surface energy γ must also be a function of temperature and strain rate.

A decrease in σ_T, the fracture strength in tension, has been reported by Congleton and Petch (refs 22 and 23) with increasing temperature for Al_2O_3, MgO, and glass. These authors attribute the decrease in σ_T with increasing temperature to a decrease in γ_R, the fracture surface energy associated with a running crack. The increase in the fracture surface energy over the intrinsic surface energy as temperature is lowered is

attributed to plastic deformation associated with crack propagation. Orowan and Irwin independently included a plastic work term in the energy balance leading to equation 1 and arrived at a modified Griffith type relationship for the conditions for crack propagation given by

$$\sigma_T \sqrt{c} = \left[\frac{2E(\gamma + \gamma_P)}{\pi} \right]^{\frac{1}{2}} \tag{4}$$

where γ_p is an energy associated with plastic work (ref 24). The fracture surface energy has also been measured as a function of crack velocity for polymethylmethacrylate and was found to first increase with crack velocity, pass through a maximum and then decrease with further increases in crack velocity (refs 25 and 26). The maximum is attributed to a change from isothermal to adiabatic conditions at the crack tip (ref 25). Although the crack velocities for our experimental conditions are unknown, the crack velocities at the low strain rate may correspond to isothermal conditions and thus be related to an increase in fracture surface energy with increasing strain rate if the results cited immediately above can be taken as typical (refs 25 and 26). However, crack velocities at the high strain rate may very well correspond to adiabatic conditions. Thus, variations of the fracture surface energy with temperature and/or strain rate may have a direct influence on the temperature and strain rate dependencies of the fracture strength. Measurement of fracture surface energy as a function of strain rate for Comp B and TNT are necessary to resolve this matter.

Slow Crack Growth

The Griffith criterion for fracture, equation 1 or its equivalent, is for catastrophic (instantaneous) crack propagation to fracture. However, many studies have shown that fracture occurs at lower stresses than the value given by equation 1 when a constant stress is maintained for a time t_f (refs 27, 28, and 29). The time t_f is generally interpreted as the time required for slow crack growth to obtain a value of crack half length, c, which will satisfy an equation like equation 1 for the constant applied stress and thus result in catastrophic crack propagation and failure. The time, t_f, is also temperature dependent and this is generally attributed to thermally activated processes (refs 27, 28, and 29). For example, Zhurkov has reported an empirical relationship of the form

$$t_f = \tau_0 e \left(\frac{U_0 - \gamma \sigma_a}{RT} \right) \tag{5}$$

where σ_a is the constant applied tensile stress, T is the temperature in degrees Kelvin, R is the ideal gas constant and τ_0, U_0 and γ are empirical constants (ref 29). Equation 5 has been found to describe the dependence of t_f and σ_a and T for about 50 different materials including metals, alloys, nonmetallic crystals and polymers (ref 29).

It is now desirable to consider the role of slow crack growth on the critical conditions for fracture as given by equation 1 or its equivalent for strain or stress which increase with time as used in the work reported here. For this purpose it is useful to introduce the stress intensity factor, K, which is given by

$$K = \sigma\sqrt{c}f \tag{6}$$

where σ is the applied stress, c is the crack half length and f is a dimensionless parameter depending on crack and sample geometry and loading conditions (ref 30). The critical stress intensity factor is the value of K - K_c for the conditions of abrupt fracture, that is

$$K_c = \sigma_c\sqrt{c_c}f \tag{7}$$

where σ_c and c_c are the critical applied stress and critical crack length that give abrupt fracture (ref 30). Equation 8 is of the same form as the Griffith condition, equation 1.

Charles (ref 31) and Evens, et. al., (refs 32 33, and 34) have considered the dependence of the fracture strength on strain rate and temperature for glass. This dependence is associated with a stress corrosion mechanism for glass but the approach is sufficiently general that it can be applied to other mechanisms than stress corrosion. The basic approach of both Charles and Evans is to start with an empirically determined relationship between the crack velocity, v, and the stress intensity factor, K, i.e., the applied stress and the crack half length (equation 6). Since empirical relationships between crack velocity and K are not available for Comp B and TNT, we proceed by assuming such a relationship, and determining its validity by comparing the predicted and observed dependencies of the fracture strength on stress rate. Thus

$$v = \frac{dc}{dt} = AK^n = A\,\sigma^n\sqrt{c^n}f^n \tag{8}$$

where

$$A = A'e^{-E/RT} \tag{9}$$

for a thermally activated process. A´ and n are constants. The same relationship of crack velocity to temperature has been used for other materials (*refs 35 and 36*).
If $\sigma = \sigma_t$, then

$$\int_{C_0}^{C_c} \frac{dc}{\sqrt{c^n}} = Af^n (\sigma)^n \int_0^{t_f} t^n dt \tag{10}$$

where c_0 is the original crack half length, c_c and t_f are the crack half length and time at fracture and σ is the stress rate. By integrating we obtain

$$\frac{2}{n-2}\left[\left(\frac{1}{c_0}\right)^{\frac{n-2}{2}} - \left(\frac{1}{c_c}\right)^{\frac{n-2}{2}}\right] = \frac{Af^n(\sigma)^n t_f^{n+1}}{n+1} \tag{11}$$

for $n \neq 2$. For $n = 2$ the solution is

$$1n\frac{c_c}{c_0} = \frac{Af^2(\sigma)^2 t_f^3}{3} \tag{12}$$

Then we obtain

$$\sigma_c = \sigma t_f = (\sigma)^{\frac{1}{n+1}}\left[\frac{2(n+1)\left[\left(\frac{1}{c_0}\right)^{\frac{n-2}{2}} - \left(\frac{1}{c_c}\right)^{\frac{n-2}{2}}\right]}{(n-2)A'f^n}\right]^{\frac{1}{n+1}} e^{\frac{E}{(n+1)RT}} \tag{13}$$

for $n \neq 2$, and for $n = 2$

$$\sigma_c = \sigma t_f = (\sigma)^{\frac{1}{3}}\left[\frac{3\,1n\left(\frac{c_c}{c_0}\right)}{A'f^2}\right]^{\frac{1}{3}} e^{\frac{E}{3RT}} \tag{14}$$

If $c_c >> c_0$, then for the general case of $n \neq 2$

$$1n\,\sigma_c = \left(\frac{1}{n+1}\right) 1n(\sigma) + \frac{E}{(n+1)RT} + J \tag{15}$$

where J is a constant. For the case of $n = 2$

$$1n\,\sigma_c = \frac{1}{3}\,1n\,(\sigma) + \frac{E}{3RT} + L \tag{16}$$

where L depends on c_c in addition to c_0. Since only two strain rates and so two stress rates were used in this work we have only two points to fit to equations 15 and 16 at a particular temperature for Comp B or TNT. However, Clark and Schmitt (ref 9) have reported σ_m versus σ for several stress rates and their data is plotted in figure 9 along with the two point for the present work and one point from the work of Costain and Motto (ref 8) for Comp B. For the Costain and Motto point and the two points of this investigation the temperature is 23°C. For the work of Clark and Schmitt the temperature is not given but is most probably about the same. If σ_c is taken as σ_m, then a least squares fit to data points of Clark and Schmitt gives a value of n = 1.94. Thus, these results satisfy equation 15 or equation 16 with H very insensitive to c_c and so stress rate if n = 2. These results justify the assumption of equation 8. In the integration of equation 10 to obtain equation 11 and 12 a threshold stress for the onset of slow crack growth was not considered although such a threshold is considered by Evans (ref 32) and there is experimental evidence for such a threshold in cases where slow crack growth is related to stress corrosion (refs 32, 34, and 37). The fit of the data of Clark and Schmitt to equations 12 or 13 indicates that if there is a threshold it can be neglected for their conditions of measurement. A threshold stress is not indicated in the data for glass in vacuum given by Wiederhorn, et. al. (ref 38). Stress corrosion is not thought to be active in this case. Equation 8 and the subsequent development leading to equations 14 and 15 for constant n is directly applicable only to Region I as discussed by Evans (ref 32). Region II and so Region III are directly related to the process of stress corrosion and are apparently only observed in cases of stress corrosion (refs 32 and 38). For Comp B and TNT there is no evidence for or against stress corrosion at this time. Measurements in controlled atmospheres and/or measurements of crack velocity is a function of the stress intensity factor, K, are necessary to resolve this matter.

For the two points of the present work a value of n = 12.5 is obtained. Charles obtained a value of n = 16 for Corning 0080 lime glass in saturated water vapor at room temperature while Evans obtained a value of n = 16 for soda lime glass in water and n = 31 for alumina in air at 50% relative humidity, both at 25°C. The somewhat large value of n obtained by both Charles and Evans for glass is thought to be related to the corrosive action of water vapor on the crack growth as effected by stress (refs 28 and 29). The crack growth rate in alumina is also apparently related to the presence of water vapor (ref 32). As pointed out by Charles a smaller value of n means more slow crack growth before reaching the critical conditions for rapid crack propagation and fracture (e.g., the Griffith criteria given by equation 1 and so a larger value of c_c and a smaller value of σ_c as observed (fig. 9). The reasons for apparently different values of n and so slow crack growth for the data of Clark and Schmitt and the results of the present investigation are not understood at this time.

The values of n obtained from the data for Comp B given in figure 5 at 0°C and 60°C are essentially the same as the value obtained at 23°C and the value at 40°C is slightly higher, i.e., n = 16. The larger value of n at 40°C is due to the low value of the compressive strength at the high rate at this temperature (fig. 5). The values of n for TNT from the data of figure 8 are about 11 for 23°C, 40°C, and 60°C but a much higher value is obtained at 0°C. An inspection of figure 8 reveals that the compressive strengths given at 0°C and the high rate may be low considering the trend as a function of temperature. The large value of n is due to the low values of σ_m at 0°C at the high rate. In general, the low rate compressive strength data of this investigation are in agreement with the values reported by Costain and Motto (ref 8) (figs. 5 and 7).

The low rate compressive strengths found in the work of this paper were obtained by the use of closed loop constant strain rate conditions. Thus, the stress rate was constant over the linear portion of the stress versus strain curve and so almost to failure (fig. 2). The high rate work was also done in closed loop but the movable crosshead was driven at the maximum possible velocity. The strain rate and so the stress rate were constant after the initial acceleration for most of the stress versus strain curve (figs. 1 and 3). The apparatus used by Costain and Motto should give a constant strain rate, but for the apparatus used by Clark and Schmitt neither the strain rate nor the stress rate are controlled. The apparatus used by these investigators was also used by the present authors to study the mechanical properties of propellants and the apparatus is described briefly in reference 40. An inspection of figure 3 of reference 40 will reveal that the slopes of the load and deflection versus time curves are approximately constant after the initial acceleration for the high rate conditions. Thus, the strain and stress rates were most probably roughly constant for the high rate work of Clark and Schmitt. However, it is not clear how the procedure and/or the apparatus was modified by Clark and Schmitt to vary the stress rate to obtain the data as a function of rate (ref 9). Thus, no information is available on the profiles of stress (and strain) versus time curves for the lower stress rates of figure 9 (lower three points). Possible differences between constant stress rate and constant strain rate are discussed by Evans (ref 32). It seems as if either a different mechanism accounts for the stress rate dependence of σ_m for the samples of Comp B used by Clark and Schmitt (n = 2) and the mechanism operative in the samples used in this study (n = 12.5), or the samples used by Clark and Schmitt for the lower stress rate measurements contained significantly larger cracks (larger c_0) than the samples used for the higher rate measurements. Clearly, additional experimental work is required to resolve this matter.

Equations 13 and 14 indicate a decrease in σ_c with increasing temperature at constant stress rate as observed (figs. 5 and 8). Equation 13 can be fitted approximately to the data for Comp B of figure 7 as a function of temperature for the low and high rates to give a value of E ≈ 30 kcal/M. This equation can also be fitted to the

low and high rate data for TNT of figure 7 if the data points at 0°C and high rate are omitted to give a value of E ≈ 36 kcal/M. These values of E are of limited significance because of the limited numbers of measurements and the limited number of temperatures available to be used in the curve fitting process. However, they are close to the activation energies reported for thermal decomposition of Comp B and TNT, i.e., 39 kcal/M and 27 kcal/M, respectively (refs 41 and 42) and so suggest a relationship between crack growth and bond breaking which is also implicit in the work of Zhurkov (ref 29). This investigator has discussed his experimental results in terms of stress assisted thermally activated bond breaking.

Wiederhorn, et. al. (ref 38) have analyzed their results of slow subcritical crack growth as a function of stress (stress intensity factor K) and temperature for glass in vacuum in terms of stress assisted thermally activated bond breaking and have arrived at a theoretical relationship between these quantities as

$$v = v_0 e^{\frac{(-E + bK)}{RT}} \tag{17}$$

where

$$b = \frac{2}{3} \frac{\Delta V}{\sqrt{\pi \rho}} \tag{18}$$

for the conditions of applied tensile stress and a through elliptical crack. E is the activation energy, ΔV is the activation volume and ρ is the radius of curvature at the crack tip. Wiederhorn, et. al. have fit their data to equation 17 and have obtained values for the activation energies and the activation volumes. A question to be considered is the applicability of equations 8 and 9 versus equation 17. For equation 17 the crack velocity is exponentially dependent on the stress intensity factor, K, while equation 8 gives a power law dependence. Evans (ref 32) has pointed out that both a power law and an exponential law will fit his data at constant temperature and the power law was chosen because the integration, e.g., equation 10, can in this case be carried out analytically. A power law assumption, equation 8, was chosen here for the same reason. If the exponential form is chosen the integration must be done numerically. However, the exponential form is based on theory, equation 17, whereas the power law is not. Additional experimental work is necessary to firmly establish the applicability of equation 8 to Comp B and TNT and/or to distinguish between equations 8 and 17.

Low Temperature Results

As noted in the Results Section, measurements were made at -20° and -40°C but the results were erratic and not reproducible. It is now believed these poor results may have been due to the method of temperature conditioning. Samples were placed in the

insulated chamber and solid carbon dioxide was blown in to reach the desired temperature below room temperature for conditioning. In this process the samples were undoubtedly thermally shocked, and this could cause cracking since TNT and Comp B are known to be sensitive to thermal shock (ref 43). It seems very desirable to repeat these measurements using a method of temperature conditioning which does not allow thermal shocking. This will give a wider range of temperatures for determining the applicability of the above equations and, in particular, for determining activation energies and whether they are related to the bond breaking processes active in thermal decomposition. It will also give data over the remaining part of the temperature range of military interest. The apparent low values of compressive strength obtained for TNT at 0°C and high strain rate (fig. 8) are most probably also due to the effect of thermal shocking.

Crack Generation and Grain Boundary Sliding

Before leaving the discussion of rate sensitivity the recent work of Sinha is considered (ref 44). This investigator developed a constitutive equation for creep at constant load and them, with a few assumptions, applied it to constant strain rate conditions and found agreement between the predictions and the experimental results for columnar grained polycrystalline ice. (Cast TNT has a tendency to be columnar grained). The stress versus strain curves as a function of strain rate show the same dependence of the compressive strength, σ_m, and the apparent modulus, E, on strain rate as observed in this work for Comp B and TNT. The total creep strain is taken to be made up of three components: (1) an elastic term which decreases immediately upon removal of the load, (2) a delayed elastic term which decreases with time after removal of the load and (3) a viscous (plastic) term which represents a permanent deformation [illegible] The delayed elastic term is attributed to grain boundary sliding which does [illegible] to cracking and permanent strain and is grain size dependent while the viscous term is due to dislocation motion. This latter term increases with crack generation which occurs when grain boundary sliding displacement reaches a critical value. All cracks are taken to have a constant length which is equal to the grain size. A model for the crack is used in which the crack is represented as an array of dislocations (ref 45). The model thus considers crack generation and not crack growth. the resultant stress versus strain relationship is non-linear and computations were made to obtain stress versus strain curves as a function of strain rate for a fixed grain boundary size and values of other parameters determined by creep studies. The calculated compressive strengths, σ_m, can be described by a power law relationship with (strain) rate as found for Comp B (fig. 9), and the strains ε_m, are found to be relatively insensitive to strain rate. The results for ice cannot be quantitatively compared to those for Comp B and TNT because parameters obtained from creep studies are needed to make the calculations and creep

studies have not been made for these materials. The delayed elastic strain has apparently been observed by Clark and Schmitt (ref 10) for Comp B but there are no measurements or observations of plastic (permanent) uniaxial deformation that the authors are aware of. In addition, the model does not contain a criterion for fracture and no mention is made of fracture of ice except at the highest strain rate considered which is lower than the lowest strain rate used in the work reported here for Comp B and TNT. Thus, to apply the approach developed by Sinha it would be necessary to add a criterion for fracture, carry out creep studies to obtain the appropriate parameters and, in particular, to determine if there is significant plastic deformation. The average grain size must also be measured.

In summary, the observed rate and temperature dependencies of the compressive strength may in part be due to (1) the rate and temperature dependencies of the true modulus and the fracture surface energy, (2) thermally activated slow crack growth before fracture and/or (3) crack generation as proposed by Sinha. Additional studies are necessary to further understand these phenomena.

Dependence on Composition

The above discussion has not taken into consideration the effects of composition and microstructure on the compressive strength except for the discussion of the work of Sinha (ref 44). The larger compressive strength of Comp B relative to the value of TNT can be attributed at least in part to the effect of second phase particles in Comp B, i.e . RDX particles on the crack path (ref 35) and the resultant energy loss during crack propagation. TNT grain size may also play a role. The dependence of the mechanical properties of these materials on composition will be considered in a separate report (ref 46).

CONCLUSIONS

The brittle fracture of polycrystalline TNT and the composite, Composition B, at constant temperature and strain rate are adequately explained by the Griffith conditions for catastrophic crack propagation. In particular, the Griffith approach predicts the observed ratios of compressive to tensile strengths, and the general orientation of the fracture surfaces are a predicted. The temperature dependence of the compressive strength can be explained on the bases of the temperature dependence of the true modulus, and thermally activated slow crack growth to the critical value necessary for rapid crack growth to fracture, with possibly a contribution by the temperature dependence of the fracture surface energy. The dependence of compressive strength on strain rate is attributed in part to the strain rate dependence of the true modulus, in part to the rate of slow crack growth to fracture and/or to the rate of crack generation, with again a

possible contribution by the rate dependence of the fracture surface energy. Although experimental results are reported only for TNT and Comp B, these conclusions should apply to the Octols and most if not all other TNT based composites. Additional work is required in almost all areas to more firmly establish the conclusions arrived at in this work. In particular, more extensive tensile properties are desirable. Measurements at lower temperatures are also desirable to better establish thermally activated crack growth and the associated activation energies and to completely cover the temperature range of military interest. Larger numbers of measurements for each set of conditions are also very desirable. Direct measurements of (slow) crack velocity as a function of stress intensity factor and temperature would definitely aid in the interpretation of the brittle fracture of these types of materials.

Table 1. Summary of experimental results at 23°C

	RATE	Comp B	TNT
σ_m COMPRESSIVE STRENGTH (PSI)	LOW	1680	960
	HIGH	3260 ± 150	1850 ± 180
E YOUNG'S MODULUS (X 10^6 PSI)	LOW	0.36	0.25
	HIGH	0.60 ± 0.02	0.45 ± 0.07
ε_m STRAIN AT σ_m (%)	LOW	0.49	0.45
	HIGH	0.65 ± 0.1	0.58 ± 0.07

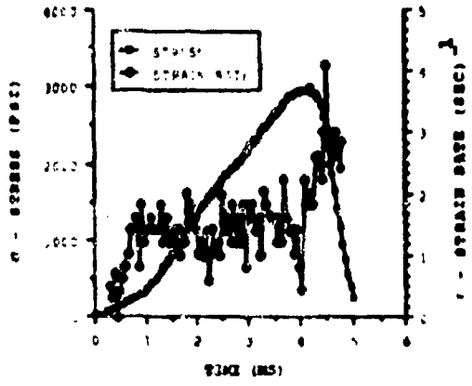

Figure 1. Typical stress and strain rate versus time for the high strain rate for Comp B at 23°C

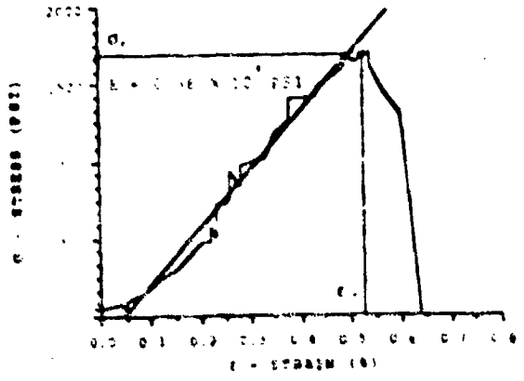

Figure 2 A stress versus strain curve for Comp B at 23°C and the low strain rate, showing the values of the compressive strength, σ_m, Young's Modulus, E, and the strain, ε_m

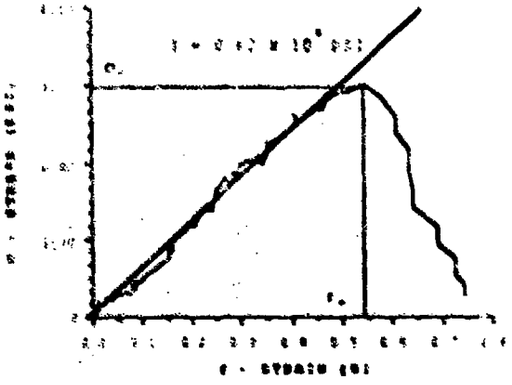

Figure 3 A typical stress versus strain curve for Comp B at 23°C and the high strain rate, showing the values of the compressive strength, σ_m, Young's Modulus, E, and the strain, ε_m

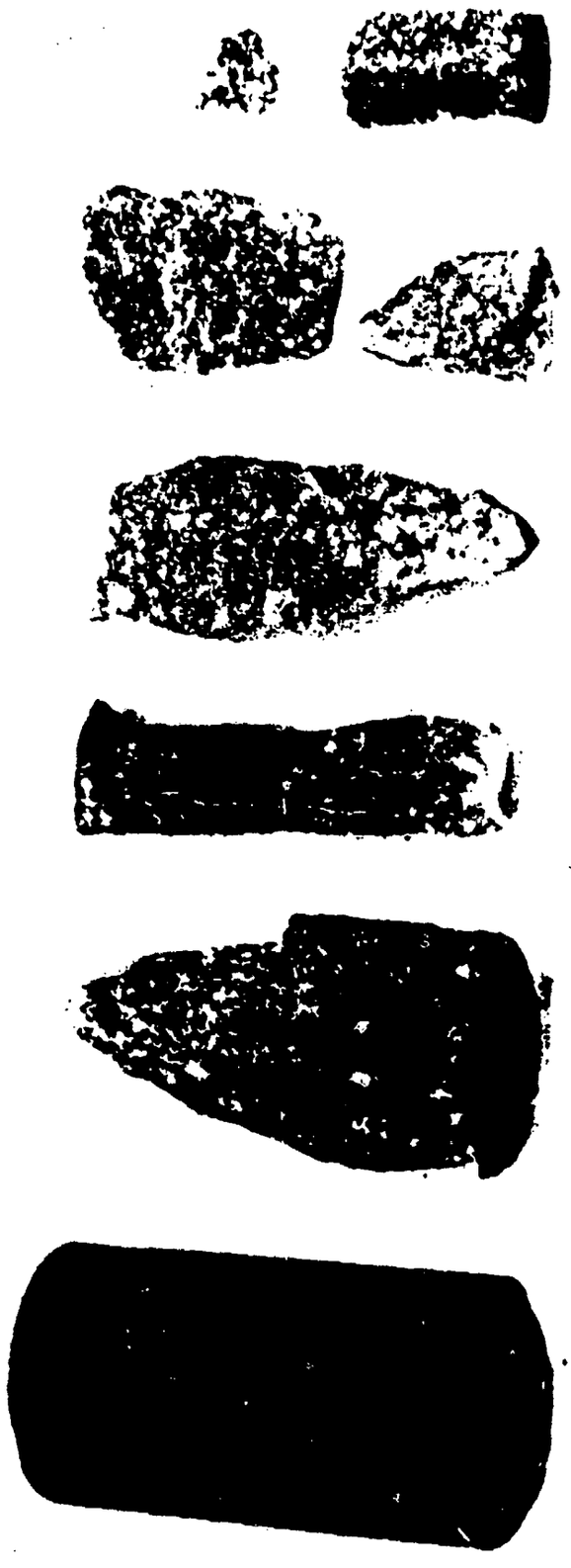

Figure 4. Typical fragments of Comp B after fracture

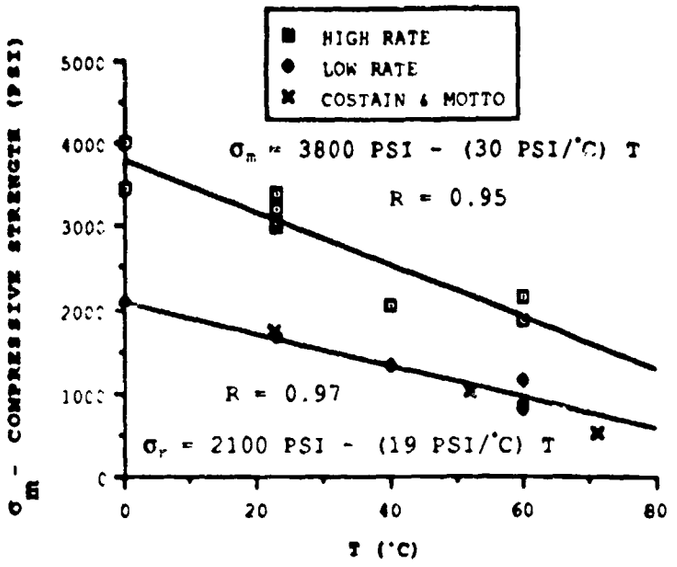

Figure 5. Compressive strength, σ_m, versus temperature for Comp B for the low and high strain rates. Also shown are points from the work of Costain and Motto (ref 8)

NOTE The lines are least squares fits of straight lines to the data points. R is the correlation coefficient (ref 7).

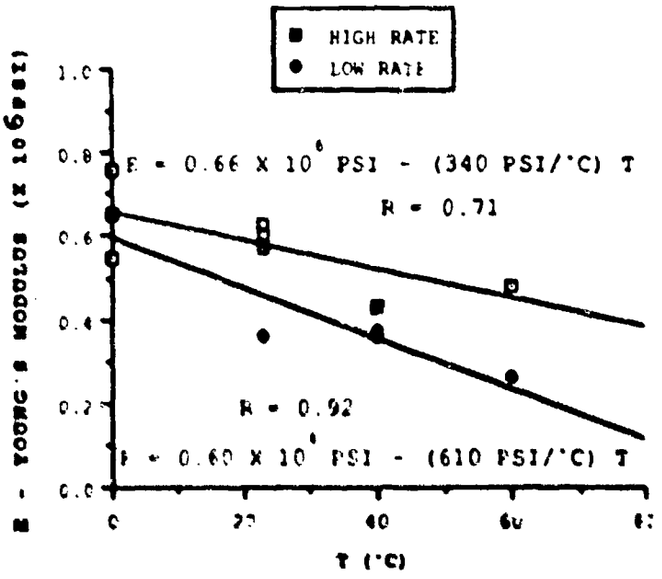

Figure 6 Young's Modulus, E, versus temperature for Comp B at the low and high strain rates.

NOTE The lines are least squares fits of straight lines to the data points. R is the correlation coefficient (ref 7)

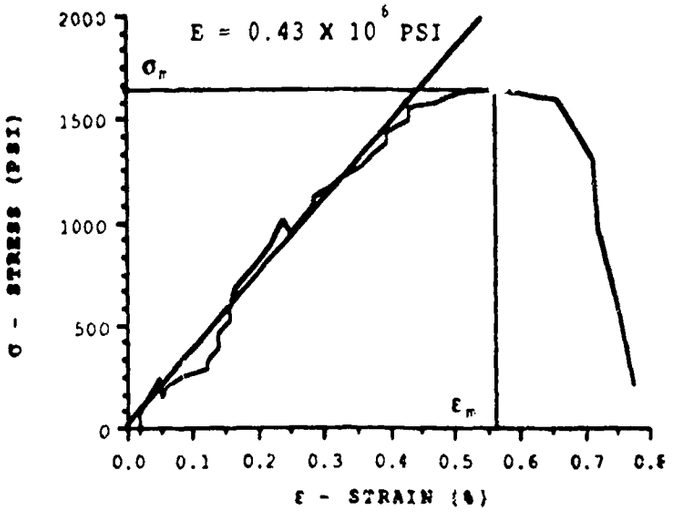

Figure 7. A typical stress versus strain curve for TNT at 23°C and the high strain rate, showing the values of the compressive strength, σ_m, Young's Moduius, E, and the strain, ε_m

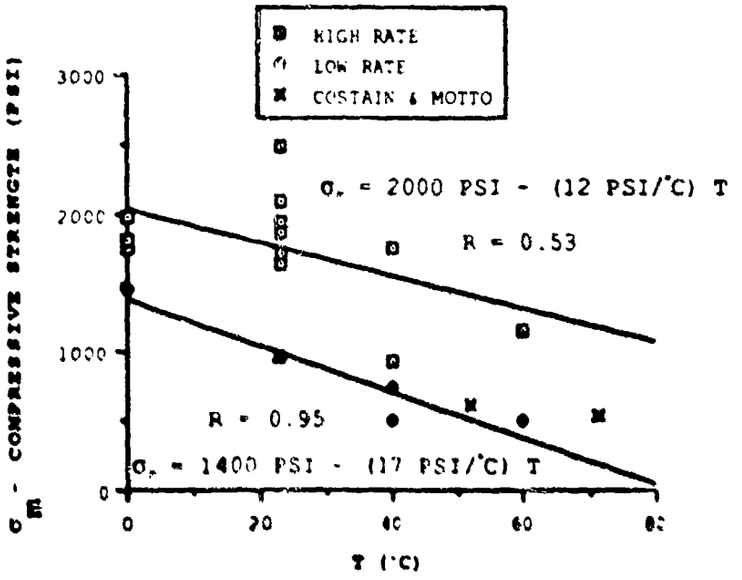

Figure 8. Compressive strength, σ_m, versus temperature for TNT for the low and high strain rates. Also shown are points from the work of Costain and Motto (ref 8).

NOTE The lines are least squares fits of straight lines to the data points. R is the correlation coefficient (ref 7)

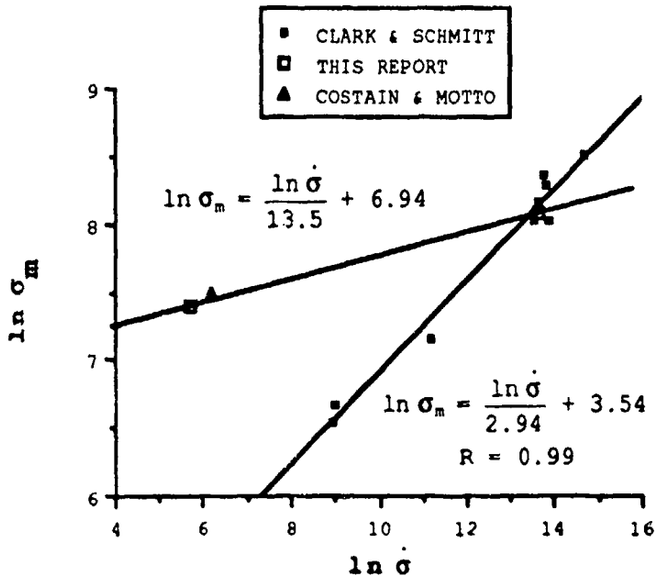

Figure 9. The natural logarithm of the compressive strength, σ_m, versus the natural logarithm of the compressive stress rate, $\dot{\sigma}$, for Comp B. Data are presented from the work of Clark and Schmitt (ref 9), from the work of Costain and Motto (ref 8), and from the present investigation.

NOTE: The line through the data of Clark and Schmitt is a least squares fit of a straight line to the data points. A straight line is also drawn through the two data points of the present investigation. R is the correlation coefficient (ref 7).

REFERENCES

1. Pinto, J. and Wiegand, D. A., to be published.

2. Pinto, J., Nicolaides, S., and Wiegand, D. A., "Dynamic and Quasi Static Mechanical Properties of Comp B and TNT," Technical Report ARAED-TR-85004, ARDEC, Picatinny Arsenal, NJ, 1985.

3. Mezger, M., unpublished results.

4. Mezger, M. and Wiegand, D. A., unpublished results.

5. Lanzerotti, M. Y. D. and Sharma, J., Appl. Phys. Lett., 39, 5, 1981.

6. Georgevich, D., private communication.

7. Papoulis, A., Probability, Random Variables, and Stochastic Processes, McGraw-Hill, NY, Second Edition, p. 150, 1984.

8. Costain, T. and Motto, R., "The Sensitivity, Performance, and Material Properties of Some High Explosives Formulations," Technical Report 4587, Picatinny Arsenal, NJ, 1973.

9. Clark, N. and Schmitt, R., Engineering Sciences Division Information Report No. 558, Picatinny Arsenal, NJ, 1972.

10. Clark, N. and Schmitt, F., unpublished report.

11. U.S. Naval Ordnance Laboratory NAVORD Report 4537 (as quoted by Clark and Schmitt (ref 9).

12. Dobratz, B. M. and Crawford, P. C., LLNL Explosive Handbook, Properties of Chemical Explosive Simulants, UCRL-52997, pp 7-8, 1985.

13. U.S. Naval Ordnance Laboratory, NAVORD Report 4380, 1956.

14. Wiegand, D. A. and Pinto, J., to be published.

15. Griffith, A. A., Phil. Trans. Roy. Soc. (London) Ser. A 221 163, 1921.

16. Griffith, A. A., Proceedings of the International Congress on Applied Mechanics, Delft, p. 55, 1924.

17. Werker, R. E., "Annotated Tables of Elasticity and Strength," Petroleum Branch, AIME, NY, 1956.

18. Costain, T., private communication.

19. Obert, L., "Brittle Fracture of Rock," in Fracture, vol. VII, ed. Liebowitz, H., Academic Press, NY, pp. 143-148, 1972.

20. Sack, R. A., Proc. Phys. Soc. (London) 58, 729, 1946.

21. See reference 20, pp 261-281.

22. Cogleton, J. and Petch, N. J., Intern. J. Fracture Mechanics, 1, 14, 1965.

23. McClintock, F. A. and Walsh, S. B., Proceedings of the 4th U.S. National Congress on Applied Mechanics, vol 2, p. 281, 1962.

24. Orowan, E., "Proceedings of the International Conference in Physics," vol 2, p. 281, Physics Society, London.

25. Vincent, P. I. and Gotham, K. V., Nature, 210, 1254, 1966.

26. Berry, J. P., "Fracture in Polymeric Glasses," Fracture, Liebowitz, H., Acedemic Press, NY, vol. VII, p. 65, 1972.

27. Bueche, F., J. Appl. Phys., 28, 784, 1957.

28. Charles, R. J., J. Appl. Phys., 29, 1549 and 1554, 1958.

29. Zhurkov, S. N., Inter. J. Fracture, 1, 311, 1965.

30. Ewalds, N. L. and Wanhill, R. S. H., Fracture Mechanics, Edward Arnold LTT., Baltimore, 1984.

31. Charles, R. J., J. Appl. Phys., 29, 1656, 1958.

32. Evans, A. G., Inter. J. Fracture, 10, 251, 1974.

33. Wiederhorn, S. M., Evans, A. G., Fuller, E. R.; and Johnson, H., J. Am. Ceramic Soc., 57, 319, 1974.

34. Wachtman, J. B., Jr., J. Am. Ceramic Soc., 57, 509, 1974.

35. Chen, E. P. and Hasselman, D. P. H., J. Am. Ceramic Soc., 59, 525, 1976.

36. Hasselman, D. P. H. and Chen, E. P., J. Am. Ceramic Soc., 60, 76, 1977.

37. Wiederhorn, S. M. and Bolz, L. M., J. Am. Ceramic Soc., 53, 543, 1970.

38. Wiederhorn, S. M.; Johnson, H.; Diness, A. M.; and Heuer, A. H., J. Am. Ceramic Soc., 57, 336, 1974.

39. Wiederhorn, S. M., J. Am. Ceramic Soc., 50, 407, 1967.

40. Nicloadies, S.; Wiegand, D. A.; and Pinto, J., "The Mechanical Behavior of Gun Propellant Grains in Interior Ballistics," Technical Report ARLCD-TR-82010, ARDEC, Picatinny Arsenal, NJ, 1982.

41. Harris, J., Thermochimica Acta, 14, 183, 1976.

42. Harris, J., private communication.

43. Joyce, M., private communication.

44. Sinha, N. K., J. Mater Sci., 23, 4415, 1988.

45. Nicolson, P. S., High Temp. Sci., 13, 279, 1980.

46. Pinto, J. and Wiegand, D. A., to be published.

DISTRIBUTION LIST

Commander
Armament Research, Development and Engineering Center
U.S. Army Armament, Munitions and Chemical Command
ATTN: SMCAR-IMI-I (5)
SMCAR-AEE, J. Lannon
SMCAR-AEE-B, D. Downs
S. B. Bernstein
E. Costa
SMCAR-AEE-BR, J. Beardell
SMCAR-AEE-W, M. Kirschenbaum
N. Slagg
SMCAR-AEE-WW, B. Fishbrun
J. Pinto (2)
M. Mezger
M. Y. Lanzerotti
D. Wiegand (15)
SMCAR-AES, S. Kaplowitz
SMCAR-AET-M, A. Rupel
S. Cytron
SMCAR-CCH-V, J. Hildebrant
Picatinny Arsenal, NJ 07806-5000

Commander
U.S. Army Armament, Munitions and Chemical Command
ATTN: AMSMC-GCL (D)
AMSMC-PBM, A. E. Siklosi
D. Fair
AMSMC-QAR-R, L. Manole
E. Bixon
Picatinny Arsenal, NJ 07806-5000

Administrator
Defense Technical Information Center
ATTN: Accessions Division (12)
Cameron Station
Alexandria, VA 22304-6145

Director
U.S. Army Materiel Systems Analysis Activity
ATTN: AMXSY-MP
AMXSY-D
Aberdeen Proving Ground, MD 21005-5066

Commander
Chemical Research, Development and Engineering Center
U.S. Army Armament, Munitions and Chemical Command
ATTN: SMCCR-MSI
SMCCR-SPS-IL
Aberdeen Proving Ground, MD 21010-5423

Commander
Chemical Research, Development and Engineering Center
U.S. Army Armament, Munitions and Chemical Command
ATTN: SMCCR-RSP-A
Aberdeen Proving Ground, MD 21010-5423

Director
Ballistic Research Laboratory
ATTN: AMXBR-OD-ST
AMXBR-BLT, R. Frey
AMXBR-E_C, J. Starkenberg
AMXBR-BLT, P. Howe
AMXBR-TBT, R. Lieb
AMXBR-TBT, J. Rochehio
Aberdeen Proving Ground, MD 21005-5066

Chief
Benet Weapons Laboratory, CCAC
Armament Research, Development and Engineering Center
U.S. Army Armament, Munitions and Chemical Command
ATTN: SMCAR-CCB-TL
SMCAR-LCB-RA, J. Vasilakis
Watervliet, NY 12189-5000

Commander
U.S. Army Armament, Munitions and Chemical Command
ATTN: SMCAR-ESP-L
AMSMC-ESM, W. D. Fortune
AMSMC-IRD, G. H. Cowan
Rock Island, IL 61299-6000

Director
U.S. Army TRADOC Systems Analysis Activity
ATTN: ATAA-SL
White Sands Missile Range, NM 88002